Identification of Key Genes and Long Non-Coding RNA Related to Bone Metastasis in Breast Cancer by Bioinformatics Analysis

Xu Teng
Capital Medical University
Wei Huang
Capital Medical University
Tianshu Yang
Capital Medical University
Weishi Li
Peking University Third Hospital
Lin Zhou
China University of Science and Technology
Zihang Wang
China University of Science and Technology
Yajuan Feng
China University of Science and Technology
Jingyao Zhang
Chinese Academy of Medical Sciences & Peking Union Medical College Hospital of Skin Diseases and Institute of Dermatology
Xin Yin
Capital Medical University
Pei Wang
Capital Medical University
Gen Li
Capital Medical University
Hefen Yu
Capital Medical University
Zhongqiang Chen
Peking University Third Hospital
Dongwei Fan (fdw@bjmu.edu.cn)
Peking University Third Hospital https://orcid.org/0000-0002-1241-0029

Primary research

Keywords: bone metastasis, breast cancer, lncRNA–mRNA network, disease-causing gene modules

Posted Date: August 12th, 2020

DOI: https://doi.org/10.21203/rs.3.rs-49982/v1

Version of Record: A version of this preprint was published at Aging on July 5th, 2021. See the published version at https://doi.org/10.18632/aging.203211.

Abstract

Background: The molecular mechanism of bone metastasis in breast cancer is largely unknown. We aimed to find key genes and long noncoding RNAs (lncRNAs) related to the bone metastasis of breast cancer using a bioinformatic approach.

Methods: We downloaded breast cancer bone metastasis gene expression data (GSE66206) and probe annotation files from the public database Gene Expression Omnibus. Then, we analyzed the network nodes to find core driver genes. Weighted correlation network analysis was performed on the gene expression profile of breast cancer bone metastasis to identify potential pathogenic modules. We performed function and pathway enrichment analyses of the genes and lncRNAs in the breast cancer bone metastasis-related modules.

Results: Based on our results, we constructed a differentially expressed lncRNA–mRNA network related to bone metastases in breast cancer and identified core driver genes, including *BNIP3* and RP11-317-J19.1.

Conclusions: Our findings provide a theoretical foundation for explaining the intrinsic molecular mechanism of breast cancer bone metastasis.

Highlight

- We compared breast cancer bone metastasis and normal samples with bioinformatic tools
- We identified a module of differentially expressed protein-coding and lncRNA genes
- BNIP3 and RP11-317-J19.1 were associated with breast cancer bone metastases

1. Background

Breast cancer is a malignant tumor that occurs in the epithelial tissue of the breast [1]. It is one of the most common malignant tumors in women worldwide, accounting for 30% of the total incidence of tumors in women. Continuous improvements in radical mastectomy technology and the application of various targeted drugs have markedly improve the survival rate and quality of life of breast cancer patients, but tumor recurrence and metastasis are still the main prognostic factors [2]. Among patients with recurrent and metastatic advanced breast cancer, bone metastasis is the most common form of metastasis, with an incidence of 65–75%; patients with first bone metastases account for 27–50% of cases [3]. Metastases commonly occur in the thoracolumbar vertebrae, sacrum, and ribs [4]. Patients with bone metastases from breast cancer often experience bone-related events such as bone pain, pathological fractures, vertebral compression or deformation, spinal cord compression, and hypercalcemia, which seriously affect patient quality of life [5]. The purpose of this study was to identify genes and long noncoding RNAs (lncRNAs) that are related to bone metastases in breast cancer to determine the molecular mechanism of bone metastases in breast cancer. The key genes and lncRNAs

we identified provide a theoretical foundation for the intrinsic molecular mechanism of breast cancer bone metastasis.

2. Materials And Methods

Gene expression data

We downloaded gene chip expression data (GSE66206) and probe annotation files from mouse breast cancer bone metastases from the Gene Expression Omnibus (GEO) database (n = 12 normal samples and n = 12 breast cancer bone metastasis samples). The probe annotation files include all probe ID files and probe sequence files for the platform.

Preparation of the data for probe re-annotation

We downloaded the V19 version of the human protein-coding gene reference transcript sequence and lncRNA reference genomic sequence data from the GENCODE database. The probe sequences of the Affymetrix chip GPL6246 platform used for GSE66206 were downloaded from GEO.

Chip probe re-annotation

First, we used a library comprising the human protein-coding gene reference transcript sequence data and lncRNA reference genome sequence data in fasta format in GENCODE to build our database. Then, based on the constructed transcription and lncRNA libraries, we re-annotated the probe sequences of GSE66206 via the blastn algorithm in preparation for construction of the mRNA and lncRNA expression profiles. When re-annotating, we ensured that all the remaining probes met the following 3 conditions: 1) The probe sequence fell completely within the transcript sequence of the protein-coding gene (PCG) or lncRNA and matched exactly; 2) if a probe sequence aligned to the transcripts of multiple PCGs or lncRNAs, it was filtered out; and 3) each PCG or lncRNA was supported by at least 2 probe sequences.

Differential expression analysis

First, we assigned the appropriate gene symbol to each probe based on re-annotation and calculated the mean expression value for all probes corresponding to the same symbol to determine the expression value for the gene in the breast cancer bone metastasis and normal samples. The gene expression profile and lncRNA expression profile were determined using the R package limma to analyze the differentially expressed genes and differentially expressed lncRNAs between the breast cancer bone metastasis samples and normal samples; the thresholds for expression differences were fold change > 1.2 or fold change < 5/6 where $p < 0.05$. We compared the screened differentially expressed genes with related genes on the National Center for Biotechnology Information (NCBI) database to obtain verified genes or potential genes.

Construction of an interaction network related to bone metastasis in breast cancer

The Spearman correlation coefficient was calculated from the gene and lncRNA expression data of the breast cancer bone metastasis and normal samples, and a rank-sum test was performed to construct a differentially expressed lncRNA–mRNA interaction network for breast cancer bone metastases (coefficient $|r| \geq 0.3$, $p < 0.05$ determined by rank-sum test). We visualized the network and analyzed the node degrees to find the core driving genes.

Weighted correlation network analysis of co-expression

Co-expression analysis of all genes and lncRNAs associated with breast cancer bone metastasis was performed with the weighted correlation network analysis (WGCNA) R package. We used the WGCNA algorithm to mine co-expressed gene modules, and then analyzed the associations between these modules and the sample phenotype. The identified breast cancer metastasis-related modules were displayed in the network using Cytoscape.

Functional enrichment analysis of the gene modules

The functions and pathways of the breast cancer bone metastasis-related and differentially expressed genes and lncRNAs were enriched with KOBAS and Enrichr, respectively.

3. Results

Screening of differentially expressed genes

The differentially expressed genes and lncRNAs in 12 breast cancer bone metastasis samples and 12 normal samples were identified using the R limma package for differential expression. We used breast cancer bone metastasis expression profile GSE66206. A total of 133 differentially expressed genes and 23 differentially expressed lncRNAs (fold change > 1.2 or fold change < 5/6) were identified. Among them, 27 genes and 3 lncRNAs were significantly differentially expressed ($p < 0.05$).

Constructing an interaction network related to bone metastasis in breast cancer

We calculated Spearman correlation coefficients for the co-expression of PCGs and lncRNAs, which we corrected using the rank-sum test. We identified 747,870 PCG–lncRNA, PCG–PCG, and lncRNA–lncRNA interactions, of which 7,451 were differentially expressed PCG–lncRNA interactions ($|r| \geq 0.3$, $p < 0.05$). We then visualized the network (Fig. 1A) and analyzed the node degrees. The Cytoscape analysis revealed that the degree of the network nodes ranged from 1 to 905. In order to identify the hub nodes in the network, we set the threshold to 20 and extracted all possible core driver genes. Twenty-eight different core driver genes were identified (Fig. 1B and Table 1). We also identified regulatory interactions between some differentially expressed genes and lncRNAs (Fig. 1C). We consulted the Human Protein Atlas Interactive Analysis to validate the protein and RNA levels of the core driver genes in breast cancer, including the levels of *IDI1*, *BNIP3*, *IFRD1*, *COQ10B*, and *ZBTB10* (Fig. 2). Immunohistochemistry and RNA expression analysis indicated that *IDI1*, *BNIP3*, *IFRD1*, and *ZBTB10* were significantly differentially expressed in cancer and healthy tissues.

Table 1
The Gene Ontology annotation of the core driver genes of breast cancer bone metastasis.

Gene symbol	Gene ID	Biological Process (GO)
CSPP1	79848	GO:0051781 positive regulation of cell division
COQ10B	80219	GO:0006743 ubiquinone metabolic process
FLVCR1	28982	GO:0043249 erythrocyte maturation
IDI1	3422	GO:0050993 dimethylallyl diphosphate metabolic process
PTP4A1	7803	GO:0030335 positive regulation of cell migration
ODC1	4953	GO:0009445 putrescine metabolic process
JMJD1C	221037	GO:0033169 histone H3-K9 demethylation
GABRB2	2561	GO:0071420 cellular response to histamine
IRF1	3659	GO:0034124 regulation of MyD88-dependent toll-like receptor signaling pathway
KDM6B	23135	GO:0071557 histone H3-K27 demethylation
IFRD1	3475	GO:0048671 negative regulation of collateral sprouting
RBM25	58517	GO:0000381 regulation of alternative mRNA splicing, via spliceosome
NCOA4	8031	GO:0006879 cellular iron ion homeostasis
SERPINA1	5265	GO:0048199 vesicle targeting, to, from or within Golgi
HSPB1	3315	GO:0038033 positive regulation of endothelial cell chemotaxis by VEGF-activated vascular endothelial growth factor receptor signaling pathway
BNIP3	664	GO:1902109 negative regulation of mitochondrial membrane permeability involved in apoptotic process
LARP4	113251	GO:0034250 positive regulation of cellular amide metabolic process
UXT	8409	GO:0047497 mitochondrion transport along microtubule
ABHD2	11057	GO:0048240 sperm capacitation
LAMTOR1	55004	GO:0060620 regulation of cholesterol import
MRPL51	51258	GO:0070126 mitochondrial translational termination
ELF2	1998	GO:0050855 regulation of B cell receptor signaling pathway
TPD52	7163	GO:0030183 B cell differentiation
PAQR5	54852	GO:0048477 oogenesis

WGCNA of co-expression

Gene expression profiles for 1,533 PCG and lncRNA genes related to breast cancer bone metastases were constructed with the WGCNA R package to build a co-expression network (merge Cut Height = 0.25, verbose = 3). The optimal threshold for the WGCNA was 12 (Fig. 3A). The sample clustering chart is shown in Fig. 3B. We excavated 5 modules from the breast cancer bone metastasis gene expression profile, including the blue (112 genes), turquoise (1,274 genes), brown (37 genes), yellow (20 genes), and grey (90 genes) modules (Fig. 3C). The results of the co-expression analysis are shown in Fig. 3D. The relationships between the various modules and traits related to bone metastases in breast cancer are shown in Fig. 3E. The genes in the yellow module are related to the disease characteristics of breast cancer bone metastases and breast cancer. In addition, the occurrence of bone metastases positively correlated with the expression of the genes in the yellow module.

Functional enrichment analysis and verification

The yellow module comprises 14 genes (Table 2). We used KOBAS to perform functional enrichment analysis using gene ontology (GO) and Kyoto Encyclopedia of Genes and Genomes (KEGG) for the genes in the yellow module [6]. With a significance threshold of $p < 0.05$, we identified 7 significant KEGG functional pathways, which revealed that the core genes in the yellow module are enriched in the prolactin signaling pathway [7] (Fig. 4A). GO enrichment analysis revealed 300 related GO functions ($p < 0.05$) involving a large number of pathways that may be related to cancer development, including regulation of signal transduction (GO: 0009966, $p = 0.00017$), cellular processes (GO: 0009987, $p = 0.00024$), cellular communication regulation (GO: 0010646, $p = 0.00030$), and positive regulation of biological processes (GO: 0048518, $p = 0.000826$) (Fig. 4B).

Enrichr was used to enrich the KEGG and GO functions of the 5 lncRNAs in the yellow module ($p < 0.05$). Some pathways enriched for the lncRNAs were related to amino acid transport (Fig. 4C and D), including alanine transport (GO: 0015808, $p = 0.00249$) and amino acid transmembrane transport (GO: 0003333, $p = 0.00747$). We identified the GABAergic synapse ($p = 0.02205$) in the lncRNA-enriched KEGG pathway, which is closely related to breast cancer metastasis [8, 9]. Therefore, the yellow module is likely to be a pathogenic module.

The lncRNA RP11-317-J19.1 and the gene *PTP4A1* act on the gene BNIP3, which plays a key role in cell apoptosis and autophagy (Fig. 4E and F) [10–13]. The gene–lncRNA interaction diagram reveals a subtle interaction between the 5 differentially expressed genes and differentially expressed lncRNAs in the yellow module (Fig. 5A and B). To validate the gene–lncRNA interactions in the yellow module, we created gene correlation scatter plots for *IDI2-AS1* and *IDI1*, *IDI2-AS1* and *PTP4A*, *IDI2-AS1* and *BNIP3*, *PTP4A* and *IDI1*, *BNIP3* and *IDI1*, and *PTP4A* and *BNIP3* (Fig. 5C). The results revealed that expression of *BNIP3* and *PTP4A* significantly positive correlated with that of *IDI1* ($p < 0.05$), whereas expression of *BNIP3* and *PTP4A* significantly negatively correlated with that of *IDI2-AS1* ($p < 0.05$). Moreover, Kaplan Meier-plotter analysis showed that 7 genes and 2 lncRNAs in the core driver gene network and co-

expression yellow module correlated with overall survival, including *IDI1*, *PTP4A1*, *BNIP3*, *IFRD1*, *ZBTB10*, *DISP1*, *COQ10B*, *IDI2-AS1*, and *SLC38A3* (Fig. 6A–I).

Table 2
The GO annotations of the genes in the yellow module.

Gene symbol	Gene ID	Biological Process (GO)
IDI1	3422	GO:0050993 dimethylallyl diphosphate metabolic process
PTP4A1	7803	GO:0030335 positive regulation of cell migration
BNIP3	664	GO:1902109 negative regulation of mitochondrial membrane permeability involved in apoptotic process
NCKAP5	344148	GO:0007019 microtubule depolymerization
SOCS2	8835	GO:0060396 growth hormone receptor signaling pathway
ADAMTS3	9508	GO:1900748 positive regulation of vascular endothelial growth factor signaling pathway
ANXA11	311	GO:0032506 cytokinetic process
DYRK1A	1859	GO:0043518 negative regulation of DNA damage response, signal transduction by p53 class mediator
EPS8L2	64787	GO:1900029 positive regulation of ruffle assembly
DISP1	84976	GO:0007225 patched ligand maturation
WDFY3	23001	GO:0035973 aggrephagy
SLC38A5	92745	GO:1904557 L-alanine transmembrane transport
NOVA1	4857	GO:0120163 negative regulation of cold-induced thermogenesi
SLC38A3	10991	GO:2000487 positive regulation of glutamine transport

4. Discussion

By comparing the differentially expressed genes identified by our screening with genes related to breast cancer bone metastasis in the NCBI database, we identified genes with verified links to breast cancer bone metastases, such as *HSPB1* and *PRL*, in our data set, thereby validating our approach. *HSPB1* expression is associated with a variety of human cancers with poor clinical prognosis. Furthermore, the *HSPB1*-encoded protein promotes cancer cell proliferation and metastasis, while protecting cancer cells from apoptosis. In addition, prolactin promotes breast cancer bone metastasis [14–16]. Expression of the receptor for prolactin can modulate the microenvironment to induce osteoclast formation.

Through functional analysis of lncRNA RP11-317-J19.1, *PTP4A1*, and *BNIP3*, we found that the interaction pairs formed by these genes participate in programmed cell death via cell apoptosis and

autophagy [10–13]. The protein encoded by the *PTP4A1* gene is a cell signaling molecule with a regulatory role in various processes, such as cell proliferation and migration; dysregulation of the protein may also be involved in the occurrence and metastasis of cancer [17–21]. The *BNIP3* gene encodes a mitochondrial protein that contains a BH3 domain and functions as a pro-apoptotic factor. *BNIP3* silencing may be mediated by lncRNA RP11-317-J19.1, allowing the protein encoded by the *PTP4A1* gene to function normally, which may induce breast cancer cells to undergo uncontrolled proliferation and migration. *PTP4A1* is highly expressed in several cancer types, and the overexpression of *PTP4A1*, which is associated with aggressive tumor characteristics, may be regulated by the PI3K/AKT pathway [22]. *PTP4A1* expression can be regulated by microRNAs that control cellular processes in breast cancer, whereas miR-601 targets *PTP4A1* to inhibit breast cancer growth and invasion [23]. The function of BNIP3 is similar to that of PTP4A1 response to the inhibition of cancer aggressive. *PTP4A1* can be modulated by the lncRNAs HULC and RP4 in response to cellular injury [24, 25]. These findings suggest that RP11-317-J19.1, *PTP4A1*, and *BNIP3* may play crucial roles in restraining the aggressiveness of cancer, thereby serving as strong predictors of breast cancer bone metastasis.

Conclusion

Conclusions

In conclusion, we constructed a differentially expressed lncRNA–mRNA network related to bone metastases in breast cancer and identified core driver genes. We found that expression modules related to alanine transport and amino acid transmembrane transport were differentially regulated in bone metastasis and normal samples. Our results reveal key genes and lncRNAs, including *BNIP3* and RP11-317-J19.1, that are related to breast cancer bone metastasis. Our findings lay the foundation for understanding the molecular basis of breast cancer bone metastasis.

Abbreviations

lncRNA, long noncoding RNA; GEO, Gene Expression Omnibus; PCG, protein-coding gene; NCBI, National Center for Biotechnology Information; WGCNA, weighted correlation network analysis;

GO, gene ontology; KEGG, Kyoto Encyclopedia of Genes and Genomes

Declarations

Ethics approval and consent to participate

The study was authorized by the Ethics Committee of Capital Medical University, and the written informed consent was signed by each patient.

Consent for publication

All authors give consent for the publication of the manuscript in Cancer Cell International.

Availability of data and materials

The datasets used and analyzed during the current study are available from the corresponding author on reasonable request.

Competing interests

The authors declare that they have no competing interests.

Funding

National Natural Science Foundation of China (30801156 (to DW.F)); National Key Research and Development Program of China (2017YFC0113001 (to DW.F)); Fostering Young Scholars of Peking University Health Science Center (BMU2017PY015 (to DW.F)); National Natural Science Foundation of China [grant numbers 81902960 (to W.H.)]; the Natural Science Foundation of Beijing (7204241 to W.H.).

Authors' contributions

All authors contributed to the work presented in this paper. XT and DWF designed the research and supervised the project. HW, TSY, HFY and PW performed statistical analysis of data. WSL and ZQC provided support e visualization and analysis support. XT wrote the manuscript. All authors read and approved the final manuscript.

Acknowledgements

No.

References

1. M.K. Schmidt, P. Kraft, D.F. Easton, R.L. Milne, M. Garcia-Closas, J. Chang-Claude, Combined associations of a polygenic risk score and classical risk factors with breast cancer risk, J Natl Cancer Inst
   Kapoor PM, Mavaddat N, Choudhury PP, Wilcox AN, Lindstrom S, Behrens S, Michailidou K, Dennis J, Bolla MK, Wang Q, Jung A, Abu-Ful Z, Ahearn T, Andrulis IL, Anton-Culver H, Arndt V, Aronson KJ, Auer PL, Freeman LEB, Becher H, Beckmann MW, Beeghly-Fadiel A, Benitez J, Bernstein L, Bojesen SE, Brauch H, Brenner H, Bruning T, Cai Q, Campa D, Canzian F, Carracedo A, Carter BD, Castelao JE, Chanock SJ, Chatterjee N, Chenevix-Trench G, Clarke CL, Couch FJ, Cox A, Cross SS, Czene K, Dai JY, Earp HS, Ekici AB, Eliassen AH, Eriksson M, Evans DG, Fasching PA, Figueroa J, Fritschi L, Gabrielson M, Gago-Dominguez M, Gao C, Gapstur SM, Gaudet MM, Giles GG, Gonzalez-Neira A, Guenel P, Haeberle L, Haiman CA, Hakansson N, Hall P, Hamann U, Hatse S, Heyworth J, Holleczek B, Hoover RN, Hopper JL, Howell A, Hunter DJ, Investigators A, kConFab AI, John EM, Jones ME, Kaaks R,

Keeman R, Kitahara CM, Ko YD, Koutros S, Kurian AW, Lambrechts D, Marchand LL, Lee E, Lejbkowicz F, Linet M, Lissowska J, Llaneza A, MacInnis RJ, Martinez ME, Maurer T, McLean C, Neuhausen SL, Newman WG, Norman A, O'Brien KM, Olshan AF, Olson JE, Olsson H, Orr N, Perou CM, Pita G, Polley EC, Prentice RL, Rennert G, Rennert HS, Ruddy KJ, Sandler DP, Saunders C, Schoemaker MJ, Schottker B, Schumacher F, Scott C, Scott RJ, Shu XO, Smeets A, Southey MC, Spinelli JJ, Stone J, Swerdlow AJ, Tamimi RM, Taylor JA, Troester MA, Vachon CM, van Veen EM, Wang X, Weinberg CR, Weltens C, Willett W, Winham SJ, Wolk A, Yang XR, Zheng W, Ziogas A, Dunning AM, Pharoah PDP. M.K. Schmidt, P. Kraft, D.F. Easton, R.L. Milne, M. Garcia-Closas, J. Chang-Claude, Combined associations of a polygenic risk score and classical risk factors with breast cancer risk, J Natl Cancer Inst, (2020).

2. Haider MT, Smit DJ, Taipaleenmaki H. The Endosteal Niche in Breast Cancer Bone Metastasis. Front Oncol. 2020;10:335.
3. Pediconi F, Galati F. Breast cancer screening programs: does one risk fit all? Quant Imaging Med Surg. 2020;10:886–90.
4. Scimeca M, Trivigno D, Bonfiglio R, Ciuffa S, Urbano N, Schillaci O, Bonanno E. Breast cancer metastasis to bone: From epithelial to mesenchymal transition to breast osteoblast-like cells, Semin Cancer Biol, (2020).
5. Wang Z, Cheng Y, Chen S, Shao H, Chen X, Wang Z, Wang Y, Zhou H, Chen T, Lin N, Ye Z. Novel prognostic nomograms for female patients with breast cancer and bone metastasis at presentation. Ann Transl Med. 2020;8:197.
6. Chen J, Liu C, Cen J, Liang T, Xue J, Zeng H, Zhang Z, Xu G, Yu C, Lu Z, Wang Z, Jiang J, Zhan X, Zeng J. KEGG-expressed genes and pathways in triple negative breast cancer: Protocol for a systematic review and data mining. Med (Baltim). 2020;99:e19986.
7. Motamedi B, Rafiee-Pour HA, Khosravi MR, Kefayat A, Baradaran A, Amjadi E, Goli P. Prolactin receptor expression as a novel prognostic biomarker for triple negative breast cancer patients. Ann Diagn Pathol. 2020;46:151507.
8. Chen X, Pei Z, Peng H, Zheng Z. Exploring the molecular mechanism associated with breast cancer bone metastasis using bioinformatic analysis and microarray genetic interaction network, Medicine (Baltimore), 97 (2018) e12032.
9. Zhang Y, Wang D, Shen D, Luo Y, Che YQ. Identification of exosomal miRNAs associated with the anthracycline-induced liver injury in postoperative breast cancer patients by small RNA sequencing. PeerJ. 2020;8:e9021.
10. Tachtsidis A, Le AV, Blick T, Gunasinghe D, De Sousa E, Waltham M, Dobrovic A, Thompson EW. Human-specific RNA analysis shows uncoupled epithelial-mesenchymal plasticity in circulating and disseminated tumour cells from human breast cancer xenografts. Clin Exp Metastasis. 2019;36:393–409.
11. Messeha SS, Zarmouh NO, Mendonca P, Alwagdani H, Cotton C, Soliman KFA. Effects of gossypol on apoptosisrelated gene expression in racially distinct triplenegative breast cancer cells. Oncol Rep. 2019;42:467–78.

12. Lee S, Hallis SP, Jung KA, Ryu D, Kwak MK. Impairment of HIF-1alpha-mediated metabolic adaption by NRF2-silencing in breast cancer cells. Redox Biol. 2019;24:101210.
13. Campbell EJ, Dachs GU, Morrin HR, Davey VC, Robinson BA, Vissers MCM. Activation of the hypoxia pathway in breast cancer tissue and patient survival are inversely associated with tumor ascorbate levels. BMC Cancer. 2019;19:307.
14. Hachim IY, Lopez-Ozuna VM, Hachim MY, Lebrun JJ, Ali S. Prolactin hormone exerts anti-tumorigenic effects in HER-2 overexpressing breast cancer cells through regulation of stemness. Stem Cell Res. 2019;40:101538.
15. Hachim IY, Lopez-Ozuna VM, Hachim MY, Lebrun JJ, Ali S. Concomitant Expression of Prolactin Receptor and TGFbeta Receptors in Breast Cancer: Association with Less Aggressive Phenotype and Favorable Patient Outcome, Int J Mol Sci, 20 (2019).
16. MacDonald TM, Thomas LN, Daze E, Marignani P, Barnes PJ, Too CK. Prolactin-inducible EDD E3 ubiquitin ligase promotes TORC1 signalling, anti-apoptotic protein expression, and drug resistance in breast cancer cells. Am J Cancer Res. 2019;9:1484–503.
17. Glodzik D, Purdie C, Rye IH, Simpson PT, Staaf J, Span PN, Russnes HG. S. Nik-Zainal, Mutational mechanisms of amplifications revealed by analysis of clustered rearrangements in breast cancers. Ann Oncol. 2018;29:2223–31.
18. Hu JY, Yi W, Wei X, Zhang MY, Xu R, Zeng LS, Huang ZJ, Chen JS. miR-601 is a prognostic marker and suppresses cell growth and invasion by targeting PTP4A1 in breast cancer. Biomed Pharmacother. 2016;79:247–53.
19. Flores-Perez A, Marchat LA, Rodriguez-Cuevas S, Bautista VP, Fuentes-Mera L, Romero-Zamora D, Maciel-Dominguez A, de la Cruz OH, Fonseca-Sanchez M, Ruiz-Garcia E, la Vega HA. C. Lopez-Camarillo, Suppression of cell migration is promoted by miR-944 through targeting of SIAH1 and PTP4A1 in breast cancer cells. BMC Cancer. 2016;16:379.
20. Lucci MA, Orlandi R, Triulzi T, Tagliabue E, Balsari A, Villa-Moruzzi E. Expression profile of tyrosine phosphatases in HER2 breast cancer cells and tumors. Cell Oncol. 2010;32:361–72.
21. Kothari S, Cizeau J, McMillan-Ward E, Israels SJ, Bailes M, Ens K, Kirshenbaum LA, Gibson SB, BNIP3 plays a role in hypoxic cell death in human epithelial cells that is inhibited by growth factors EGF and IGF, Oncogene, 22 (2003) 4734–4744.
22. LZ L, YZ H, D. PP M, LJ W, ZC L, XY DM, LX Y, JY S, Q ZJ,FJ,G, W. XY, Protein tyrosine phosphatase PTP4A1 promotes proliferation and epithelial-mesenchymal transition in intrahepatic cholangiocarcinoma via the PI3K/AKT pathway, Oncotarget, 7 (2016) 75210–75220.
23. JY H, W Y, X W, MY Z, R X, LS Z, ZJ H, JS C. miR-601 is a prognostic marker and suppresses cell growth and invasion by targeting PTP4A1 in breast cancer. Biomed Pharmacother. 2016;79:247–53.
24. Y ZL,M. L. S, Long non-coding RNA HULC promotes UVB-induced injury by up-regulation of BNIP3 in keratinocytes. J Biomedicine pharmacotherapy. 2018;104:672–8.
25. Q RJ,XJ,L, Y W, H G, T M. Z. H, n. Chi H %J Artificial cells, biotechnology, Upregulation of long noncoding RNA RP4 exacerbates hypoxia injury in cardiomyocytes through regulating miR-

939/Bnip3/Wnt/β-catenin pathway, 47 (2019) 3013–3020.

Figures

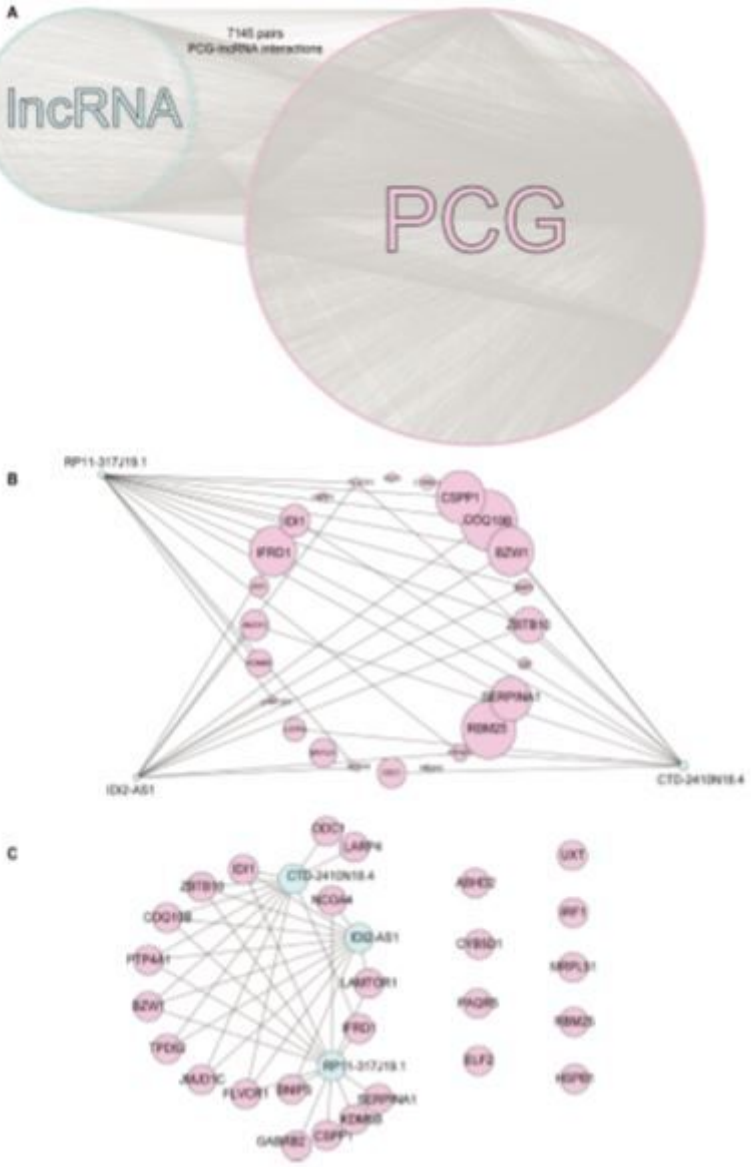

Figure 1

Network of differentially expressed PCG–lncRNA interactions. A: Network of differentially expressed PCG–lncRNA interactions. B: Core driver gene network. C: Interactions between differentially expressed genes and lncRNAs.

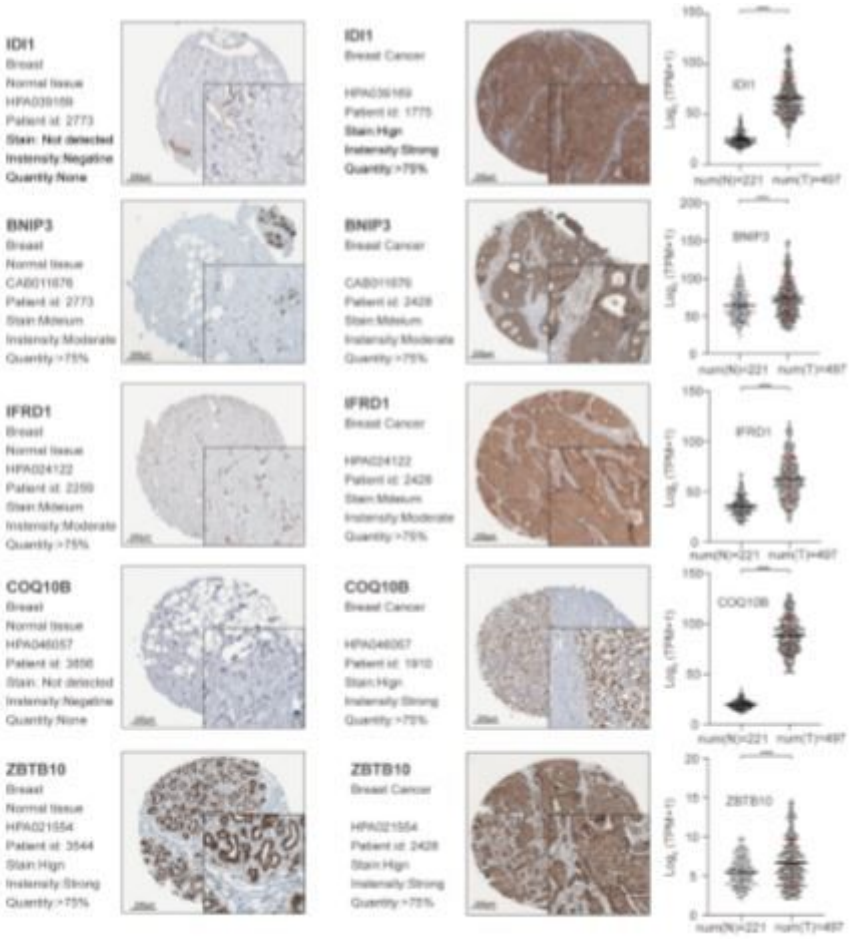

Figure 2

Validation of significant core genes in breast cancer bone metastasis by immunohistochemistry and RNA expression analysis.

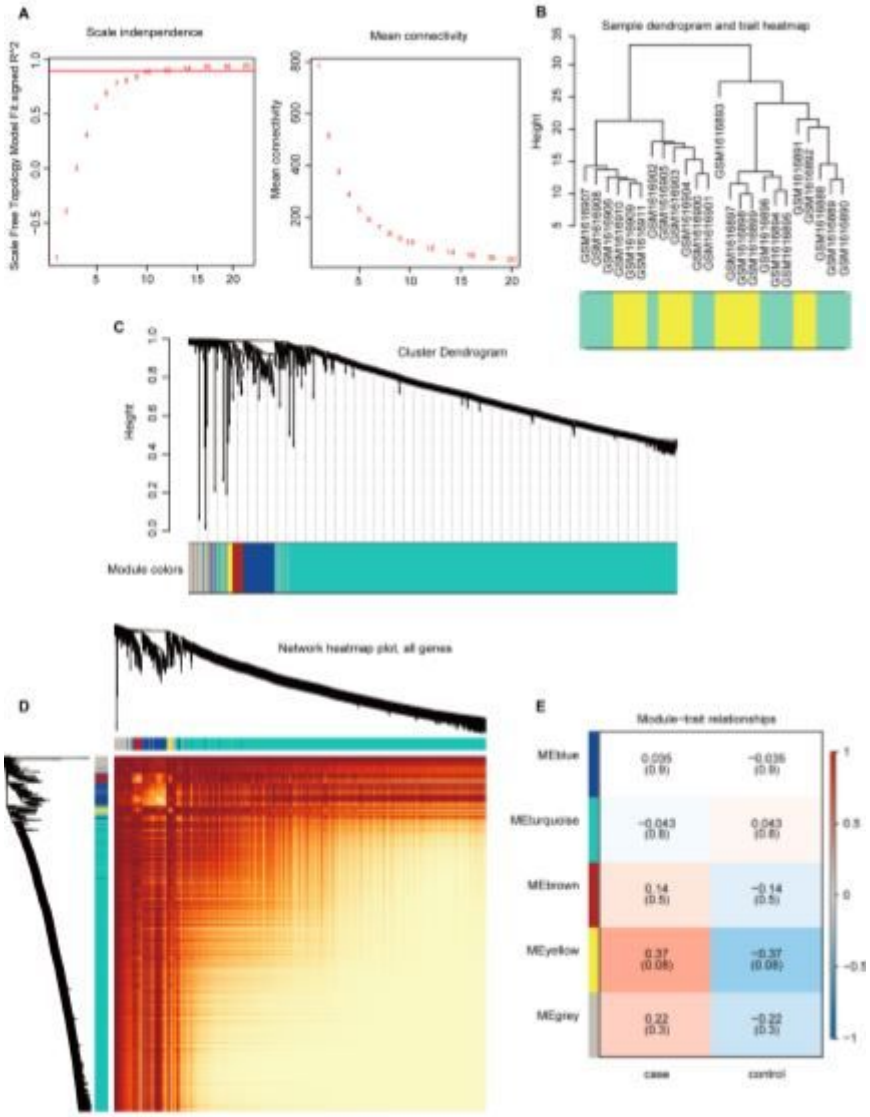

Figure 3

Construction and analysis of co-expression modules. A: Optimal threshold selection map for breast cancer bone metastasis co-expression. B: Clustering of breast cancer bone metastasis samples. C: Phylogenetic tree of module clustering. D: Co-expression analysis heat map. E: Breast cancer bone metastasis module and traits.

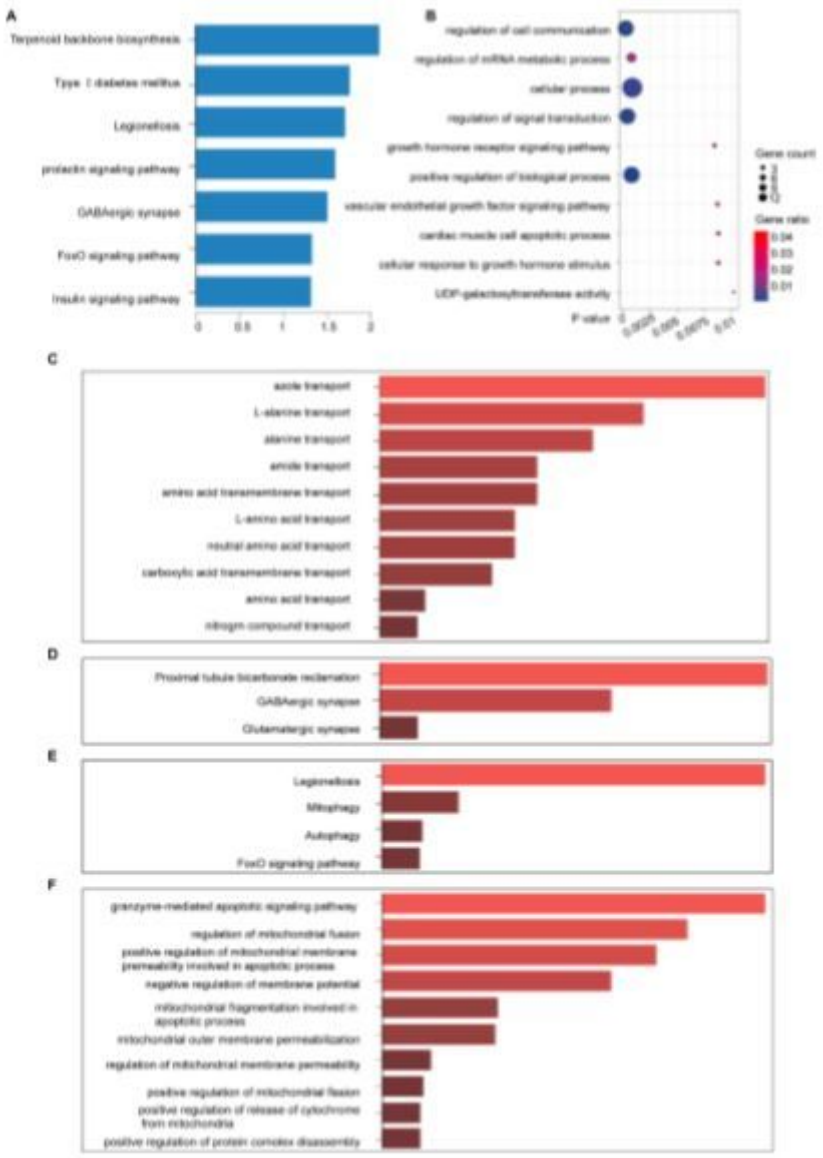

Figure 4

KEGG and GO function enrichment analysis. A: KEGG pathway enrichment in the yellow module. B: GO pathway enrichment in the yellow module. C: GO enrichment of lncRNAs in the yellow module. D: KEGG enrichment of the functions of the lncRNAs in the yellow module. E: KEGG pathway enrichment for the interactions of the differentially expressed genes in the yellow module. F: GO pathway enrichment for the interactions of the differentially expressed genes in the yellow module.

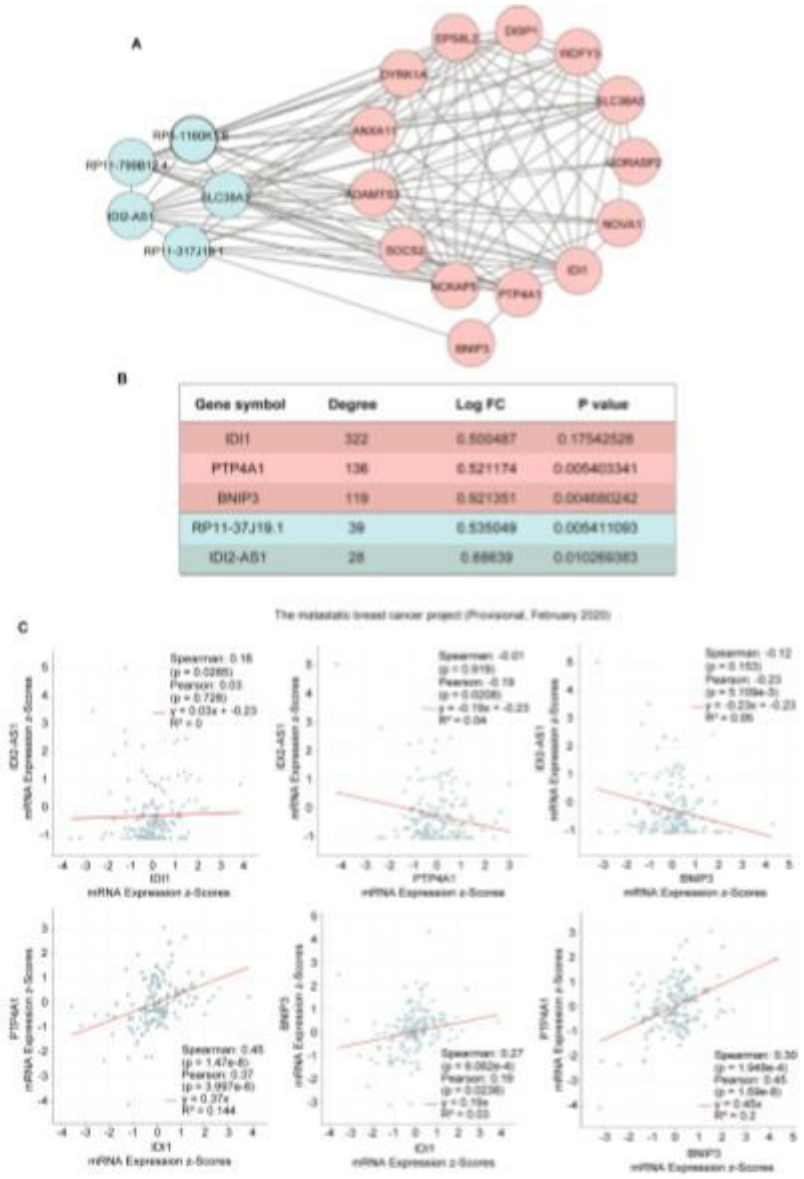

Gene symbol	Degree	Log FC	P value
IDI1	322	0.500487	0.17542528
PTP4A1	136	0.521174	0.005403341
BNIP3	119	0.521351	0.004680242
RP11-37J19.1	39	0.535049	0.005411093
IDI2-AS1	28	0.68639	0.010266383

Figure 5

Interactions of the genes in the yellow module. A: The interactions between 5 differentially expressed genes and differentially expressed lncRNAs in the yellow module. B: The 5 differentially expressed genes in the yellow module. C: Gene correlation scatter plots from the yellow module. The Pearson correlation coefficients of IDI2-AS1 and IDI1, IDI2-AS1 and PTP4A, IDI2-AS1 and BNIP3, PTP4A and IDI1, BNIP3 and IDI1, and PTP4A and BNIP3.

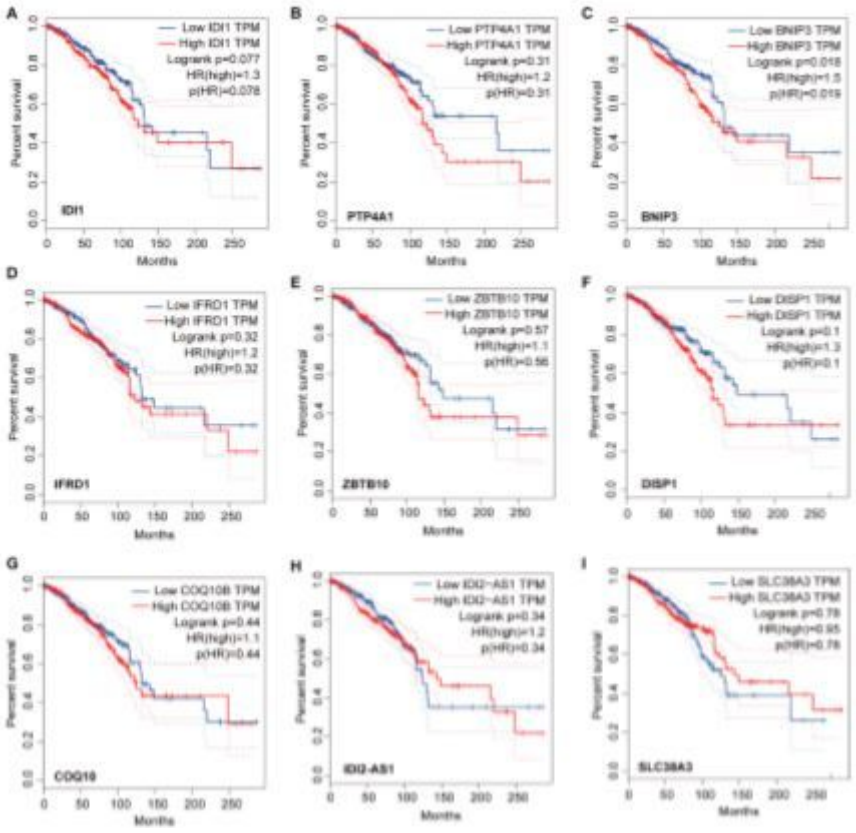

Figure 6

Analysis of overall survival based on expression of the 7 genes and 2 lncRNAs in the core driver gene network. Survival was measured by Kaplan–Meier analysis based on expression of IDI1 (A), PTP4A1 (B), BNIP3 (C), IFRD1 (D), ZBTE10 (E), DISP1 (F), COQ10 (G), IDI2-AS1 (H), and SLC38A3 (I). X-axes display survival time (Months), and y-axes display percent survival.